

A Laparoscopic Telesurgical Workstation

Murat Cenk Çavuşoğlu, Frank Tendick, Michael Cohn, and S. Shankar Sastry

Abstract—Medical robotics and computer aided surgery in general, and robotic telesurgery in particular, are promising applications of robotics. In this paper, various aspects of telesurgery are studied. After a general introduction to laparoscopic surgery and medical applications of robotics, the UC Berkeley/Endorobotics Inc./UC San Francisco Telesurgical Workstation, a master-slave telerobotic system for laparoscopic surgery, is introduced, followed by its kinematic analysis, control, and experimental results. Later some conceptual and future issues on telesurgery are discussed, including teleoperation and hybrid control, focusing on the special requirements of telesurgery.

Index Terms—Laparoscopy, medical robotics, minimally invasive surgery, telesurgery.

I. INTRODUCTION

MEDICAL robotics and computer assisted surgery are new and promising fields of study that aim to augment the capabilities of surgeons by taking the best from robots and humans.

In this joint project between the Robotics and Intelligent Machines Laboratory, University of California, Berkeley, Endorobotics Inc., and the Department of Surgery, University of California, San Francisco, a telesurgical workstation is being developed for use in laparoscopic surgery [1]. The current design is a six degree-of-freedom (DOF) manipulator, instrumented with a gripper, controlled by a six DOF master manipulator.

Research on medical robotics at UC Berkeley includes the development of an endoscopic manipulator [2], [3], early designs of millirobotic manipulators for laparoscopy [4], and studies on tactile sensing [5]–[7].

A. What is Laparoscopic Surgery?

Laparoscopic surgery is a revolutionary technique [8]. It is minimally invasive, i.e., the surgery is performed with instruments inserted through small incisions (less than 10 mm in diameter) rather than by making a large incision to expose the operation site. The main advantage of this technique is the reduced trauma to healthy tissue, which is the leading

cause of post-operative pain and long hospital stay of the patient. The hospital stay and rest periods, and therefore the procedure's cost, are significantly reduced with minimally invasive surgery, at the expense of more difficult techniques performed by the surgeon.

Minimally invasive operations include laparoscopy (abdominal cavity), thoracoscopy (chest cavity), arthroscopy (joints), pelviscopy (pelvis), and angioscopy (blood vessels). The first major laparoscopic surgery, for colecystectomy (removal of gall bladder), was performed in 1985 by Mühe in (West) Germany. In less than a decade, there was a quick shift from open surgery to laparoscopic surgery in relatively simple procedures, with 67% of cholecystectomies performed laparoscopically in the U.S. in 1993 [9]. Adoption of laparoscopic techniques has been slower in more complex procedures, largely because of the greater difficulty due to the surgeon's reduced dexterity and perception.

In laparoscopic surgery, the abdominal cavity, which is expanded by pumping carbon dioxide inside to open a workspace, is observed with a laparoscope inserted through one of the incisions. The laparoscope itself is composed of a chain of lens optics to transmit the image of the operation site to the CCD camera connected to its outer end, and optical fibers to carry light to illuminate inside. A monoscopic image of the operation site is displayed on a high resolution CRT screen. The instruments used for the operation are specially designed long and thin instruments with trigger-like handles. They are inserted through trocars placed at the incisions to air seal the abdomen. The instruments have only four DOF (see Fig. 1), preventing the ability to arbitrarily orient the instrument tip [10]. Dexterity is significantly reduced because of the lost DOF's and motion reversal due to the fulcrum at the entry point. Force feedback is reduced due to the friction at the air tight trocar and the stiffness of the inflated abdominal wall. There is no tactile sensing, on which surgeons highly depend in open surgery to locate arteries and tumors hidden in tissue.

Minimally invasive surgery itself is telemanipulation as the surgeon is physically separated from the workspace. Therefore, telerobotics is a natural tool to extend capabilities in laparoscopic surgery. With the telesurgical workstation, the goal is to restore the manipulation and sensation capabilities of the surgeon which were lost due to minimally invasive surgery. The six DOF slave manipulator, controlled through a spatially consistent and intuitive master, will restore the dexterity, the force feedback to the master will increase the fidelity of the manipulation, and the tactile feedback will restore the lost tactile sensation.

Other work in the literature on telesurgical systems for abdominal surgery include the telesurgical system for open

Manuscript received November 25, 1997; revised March 31, 1997. This paper was recommended for publication by Editor R. H. Taylor upon evaluation of the reviewers' comments. This work was supported in part by NASA under Grant STTR-NAS-1-20288, NSF under Grant IRI-95-31837, and ONR under MURI Grant N14-196001001200.

M. C. Çavuşoğlu and S. S. Sastry are with the Department of Electrical Engineering and Computer Sciences, University of California, Berkeley, CA 94720 USA.

F. Tendick is with the Department of Surgery, University of California, San Francisco, CA 94143-0475 USA. He is also with the Department of Bioengineering, University of California, Berkeley, CA 94720 USA.

M. Cohn is with Endorobotics, Inc., Berkeley, CA 94709 USA.

Publisher Item Identifier S 1042-296X(99)05400-2.

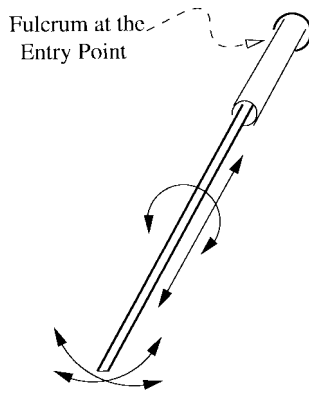


Fig. 1. Four-DOF available in conventional laparoscopic instruments.

surgery with four DOF manipulators developed at SRI International [11] (a laparoscopic version has also been developed), the telerobotic assistant for laparoscopic surgery developed by Taylor *et al.* [12], and the telesurgery experiments performed between JPL, Pasadena, CA, and Polytechnic University of Milan, Italy [13], and between Nagoya and Tokyo in Japan [14].

There are other successful medical applications of robotics, including systems for orthopedic surgery [15], microsurgery and stereotactic neurosurgery [16], eye surgery [17], and radiotherapy [18]. See [19] and [20] for good reviews.

This paper will first introduce the UC Berkeley/Endorobotics/UCSF Telesurgical Workstation, perform its kinematic analysis, give information about control issues, describe the implemented control algorithm, and present experimental results. Finally, a short discussion on conceptual and future issues on telesurgery will be presented including teleoperation and hybrid control issues.

II. DESCRIPTION OF THE SYSTEM

A. Design Requirements

The goal of the design is to add a two DOF wrist to extend the four DOF available through the fulcrum, and therefore give enough dexterity to perform complex skills, especially suturing and knot tying, in the minimally invasive setting. The slave must be small enough to fit through incisions typically 10 mm wide, but also able to apply forces large enough to manipulate tissue and suture. It must have sufficient workspace to span significant regions in the abdominal cavity and suture at almost arbitrary orientations, yet have a wrist short enough in length to work in constrained spaces. System bandwidth should permit natural motions by the surgeon and haptic feedback with sufficient fidelity. Of course, the system must be safe to be used inside a patient.

Performance goals in the design of the millirobot are given in Table I.¹ These values are estimated for a suturing task, force and movement requirements for driving a needle through tissue and tying a knot. The diameter of the instrument is chosen to fit the standard 10 and 15 mm diameter trocars. It is preferable not to have larger diameters as it causes greater

TABLE I
PERFORMANCE GOALS FOR THE MILLIROBOT

Parameter	Value
Dimension: overall diameter	10–15 mm max
Dimension: wrist joint to grasper	100 mm max
Force: at the point of needle, for driving the needle through tissue	1.5 N min
Torque: about grasper axis, for driving needle (assumes curved needle, 15 mm from grasper to needle tip)	2.2 N-cm min
Force: gripping, while driving needle	5 N min
Force: knot tightening tension	2.2 N min
Range of motion: gripper jaw opening	2–3 mm min
Range of motion: rotation about grasper axis, to drive plus allowance for inclined work surface	180–270 degrees min
Range of motion: wrist flexion, for driving needle	90 degrees min
Range of motion: wrist pronation	360 degrees min
Bandwidth	5 Hz min

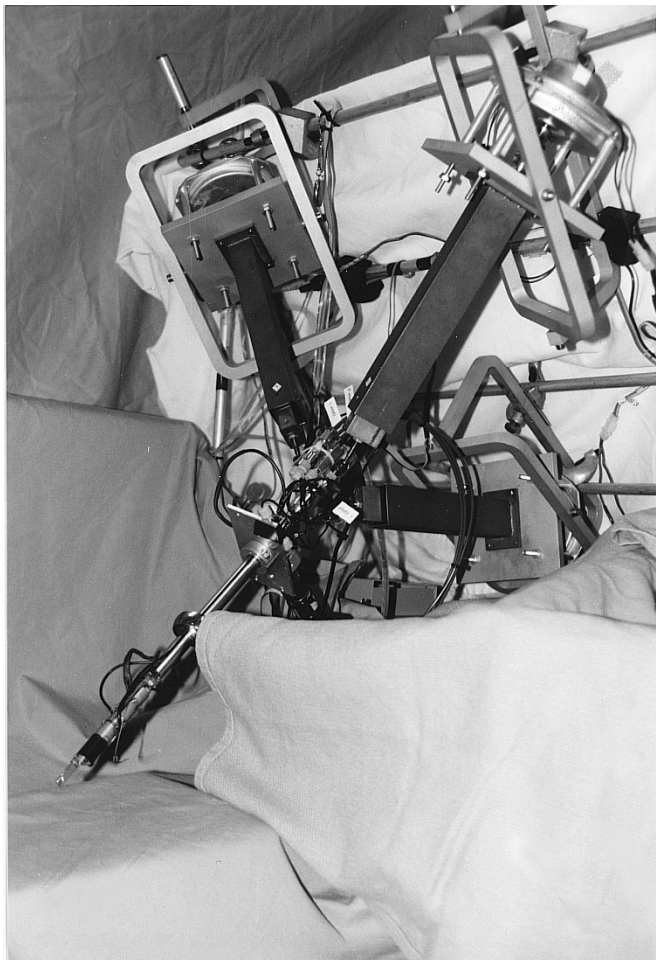
damage to healthy tissue. It is not necessary to go smaller than 10 mm for laparoscopic surgery as there are other instruments, for example staplers, that require a 10 mm trocar. The wrist-to-grasper length is determined by the clearance between the abdominal wall and the key organs when the abdomen is pressurized. Torque and force requirements are estimated from measurements on instruments performing suturing in an open surgical setting. A 270° of roll rotation is required for driving the needle through tissue in a single movement without regrabbing it. 90° of wrist flexion with 360° of gross rotation is necessary for suturing at the desired orientations. The bandwidth requirement is set to accommodate the bandwidth of intentional hand movements.

B. Current Prototype

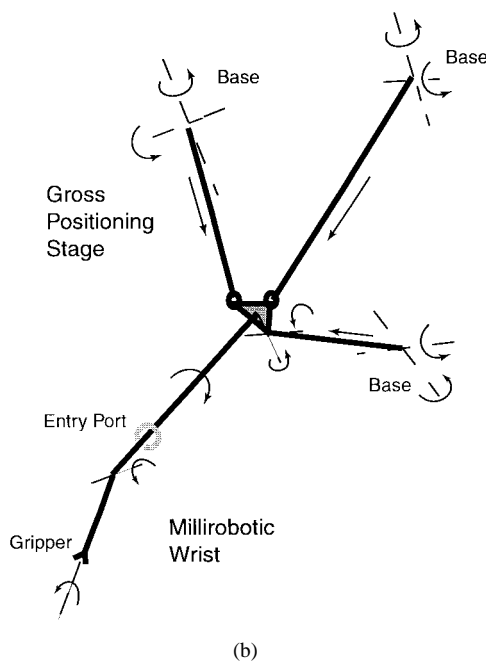
To meet the design requirements, the slave manipulator is composed of two parts (Fig. 2). The first part is the gross positioning stage located outside the body. It is responsible for positioning the millirobot, which is the second part of the slave robot. The gross stage controls the same four DOF as those available in conventional laparoscopic instruments. As the gross stage is located outside the body, there is not a tight space limitation. A parallel arrangement is chosen for increased rigidity and a small footprint. Three linear joints, which are connected to the base of the robot with gimbal arrangements, hold a small platform that carries the tool arm and the motor rotating it. Two of the linear joints are connected to the platform with three DOF ball joints whereas the third one is connected with a two DOF joint. All four actuators of the gross positioning stage are DC servo motors. In the linear joints, power is transmitted by lead screws connected to the motors. The roll axis through the entry port is direct drive.

The second part of the slave, the millirobot, is located inside the patient and consequently must be small yet capable of producing a wide range of motion and relatively large forces. To meet these requirements, it has a two DOF wrist, with yaw and roll axis rotations, and a gripper (Fig. 3). It is 10 mm in diameter. The wrist-to-gripper length is 10 cm. The yaw axis

¹ Courtesy of Endorobotics Inc.



(a)



(b)

Fig. 2. Slave manipulator of the Berkeley/Endorobotics/UCSF laparoscopic workstation.

is actuated by tendons driven by a DC servo motor located outside the body. The roll axis and the gripper are actuated



Fig. 3. Millirobotic wrist.

TABLE II
MILLIROBOT TEST RESULTS

Parameter	Measured Value	Target Value
Gripping force	15 N	5 N min
Grasper opening width	6 mm	2-3 mm min
Wrist roll torque	8.8 N-cm	2.2 N-cm min
Wrist roll range of motion	90 degrees	180-270 degrees min
Wrist flexion (yaw) torque	30 N-cm	10-15 N-cm
Bandwidth	~6 Hz	5 Hz

hydraulically through pairs of bladders which are inflated with water. The water section is separated from the rest of the hydraulic circuit, outside the body, via a set of diaphragms. The millirobot is designed to be disposable, and the bladders will be driven by sterile saline solution to avoid problems in case of leaks.

Table II gives the experimentally determined open loop performance results of the actual slave manipulator. All the design goals are exceeded except for the range of roll rotation as a result of actuator design limitations.

The master manipulator (See Fig. 4) is a six DOF serial robot. A commercial four DOF force reflecting joystick (Immersion Impulse Engine 3000) with three actuated axes is equipped with an additional two DOF (one actuated) and a stylus handle. The additional two DOF was necessary to control the six DOF slave manipulator. There are position measurements in all six joints and the four actuated joints give force feedback in translational directions and the roll axis. The torque feedback on the roll axis is especially important to feel when the needle enters and leaves the tissue while suturing. The stylus handle was chosen to give a more dextrous interface for precise manipulation.

The major safety feature present in this prototype of the system is the heartbeat check by the robot. The robot continuously monitors a heartbeat signal sent by the control program, and cuts the power to all of the actuators in case this signal is lost, which means a computer failure. Additional safety features to be implemented in the second version of the robot will be discussed later in this paper.

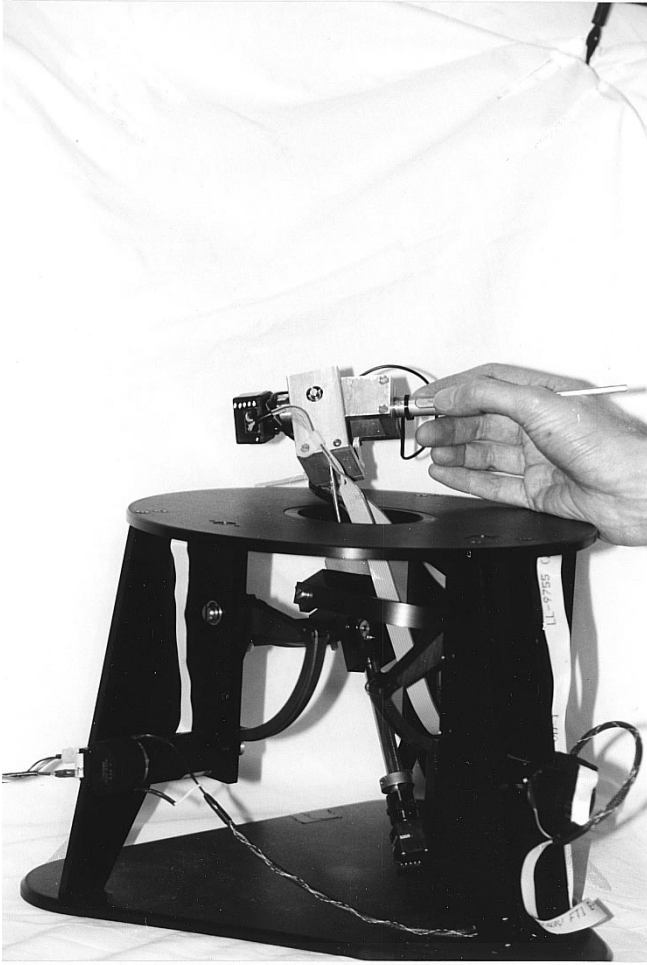


Fig. 4. Master manipulator of the laparoscopic workstation.

III. KINEMATICS

For feedforward control of the system, the inverse kinematics of the slave manipulator and the forward kinematics of the master manipulator are needed. The forward kinematics of the slave are also necessary for position error-based force feedback.

The hybrid parallel-serial structure of the slave manipulator is an unusual design which complicates the solution of the inverse kinematics. We will present the calculation of the forward kinematics of the slave manipulator to show the workspace of the robot. The details of the calculations are included as the techniques used are neither standard nor obvious. The master manipulator is a straightforward design and therefore briefly described for completeness.

For the kinematic analysis, the product of exponentials formulation is used. Refer to [21] for a full treatment.

A. Slave Manipulator Inverse Kinematics

In inverse kinematics, the problem is to solve for the joint angles² of actuated joints, given $g_{ft} \in SE(3)$, the desired configuration of the tool relative to the fulcrum.

²For brevity, we use the term *angles* to specify the values of generalized joint variables, which can be angles or lengths.

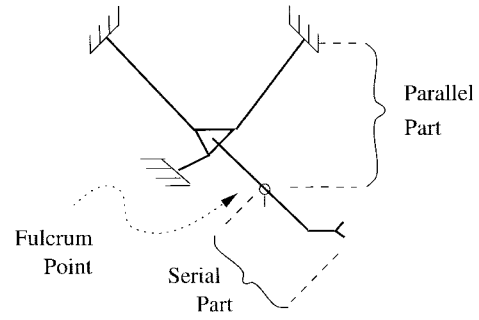


Fig. 5. Parallel and serial parts of the slave robot.

Notation: The joint variables of the actuated joints are: lengths of linear joints, l_0, l_1, l_2 , roll and yaw rotations of the millirobot, θ_1 and θ_2 , and gross stage rotation θ_0 .

To simplify the inverse kinematics calculations, the slave kinematics can be divided into two parts: the serial portion inside the body and parallel portion outside the body. The serial part is composed of the fulcrum, which is modeled with a spherical joint and a translational joint, and the two DOF wrist. The parallel part of the slave consists of the three arms holding the base of the tool arm, and the tool arm itself (Fig. 5).

In the inverse kinematics calculations, first the serial part will be solved, which will give the angles of the wrist joints and the desired configuration of the parallel part. Then the parallel part will be solved to calculate the lengths of the linear joints and the tool arm rotation.

1) *Serial Part:* Using the naming convention and the zero configuration shown in Fig. 6, the kinematic configuration of the serial part is characterized by the following twists³

$$\begin{aligned} \xi_{s1} &= e_4 & \xi_{s2} &= e_5 & \xi_{s3} &= e_6 \\ \xi_{s4} &= e_3 & \xi_{s5} &= e_5 & \xi_{s6} &= e_6 \end{aligned} \quad (1)$$

and the reference configuration

$$g_s(0) = I_{4 \times 4} \in SE(3) \quad (2)$$

which gives the forward kinematics map as

$$g_s(\theta_s) = e^{\hat{\xi}_{s1}\theta_{s1}} e^{\hat{\xi}_{s2}\theta_{s2}} e^{\hat{\xi}_{s3}\theta_{s3}} e^{\hat{\xi}_{s4}\theta_{s4}} e^{\hat{\xi}_{s5}\theta_{s5}} e^{\hat{\xi}_{s6}\theta_{s6}} g_s(0). \quad (3)$$

The inverse kinematics of the serial part is straightforward as it is a kinematically simple configuration.

Lemma 1—Inverse Kinematics of the Serial Part: Given the desired configuration

$$g_{ft} = \begin{bmatrix} R_d & p_d \\ 0 & 0 & 1 \end{bmatrix} \in SE(3) \quad (4)$$

$$\theta_{s4} = \|p_d\| \quad (5)$$

$$\theta_1 = \theta_{s5} = \text{atan2}\left(\mp\sqrt{\beta_x^2 + \beta_y^2}, -\beta_z\right) \quad (6)$$

$$\theta_2 = \theta_{s6} = \text{atan2}(-\beta_y, \beta_x) \quad (7)$$

where

$$\beta = g_d^{-1} \begin{bmatrix} 0 \\ 0 \\ 0 \\ 1 \end{bmatrix}. \quad (8)$$

³ e_i denotes the i th standard basis vector for \mathbf{R}^6 .

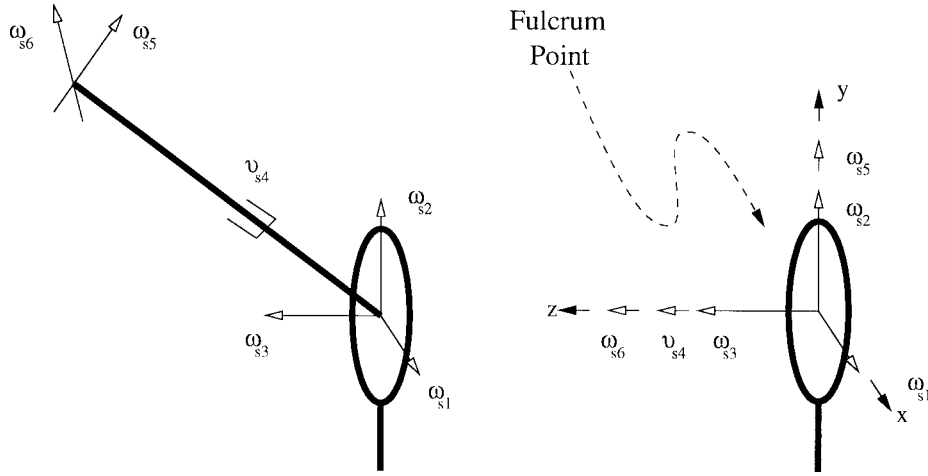


Fig. 6. Naming convention and the zero configuration of the serial part.

Here, note that θ_{s5} has two solutions, and θ_{s6} can have any value when $\theta_{s5} = 0$, which is a singular configuration.

Then

$$e^{\hat{\xi}_{s1}\theta_{s1}} e^{\hat{\xi}_{s2}\theta_{s2}} e^{\hat{\xi}_{s3}\theta_{s3}} = g_d e^{-\hat{\xi}_{s6}\theta_{s6}} e^{-\hat{\xi}_{s5}\theta_{s5}} e^{-\hat{\xi}_{s4}\theta_{s4}} \quad (9)$$

will be used in the solution of the parallel part, since ξ_{s1} , ξ_{s2} , and ξ_{s3} form the fictitious ball joint at the entry point.

2) *Parallel Part*: The parallel part of the slave consists of three arms connected to a triangular platform which holds the millirobot. Two of the arms have six DOF, whereas the third one has only five. In each of the arms, only one DOF, the translational joint, is actuated. The solution of the inverse kinematics for the parallel part requires finding the lengths of these translational joints and calculating the rotation of the tool arm. In the solution, one proceeds to solve the inverse kinematics of the five DOF arm, then uses this to calculate the lengths of the prismatic joints in the other two arms, and the amount of rotation.

Specification of the Configuration: Fig. 7 gives a side view of the parallel part, showing the joint naming conventions and various points and coordinate frames used in the calculations. In the figure, joints 1–5 are on the five DOF arm, and joint 6 is the rotation of the tool arm. The serial part of the inverse kinematics gives the direction n , which is determined from the spherical joint at the fulcrum, as

$$n_f = e^{\hat{\xi}_{s1}\theta_{s1}} e^{\hat{\xi}_{s2}\theta_{s2}} e^{\hat{\xi}_{s3}\theta_{s3}} \begin{bmatrix} 0 \\ 0 \\ 1 \\ 0 \end{bmatrix} \quad (10)$$

and the length d :

$$d = \theta_{s4}. \quad (11)$$

As notation, the subscripts of points and vectors denote the coordinate frames in which they are expressed. The subscripts of the homogeneous transforms denote which coordinate frames they transform. Also, $\langle \cdot, \cdot \rangle$ is used to denote inner product.

The forward kinematics of the 5 DOF arm, choosing the zero configuration as W overlapped with M , are

$$g_{mw}(\theta_p) = e^{\hat{\xi}_{p1}\theta_{p1}} e^{\hat{\xi}_{p2}\theta_{p2}} e^{\hat{\xi}_{p3}\theta_{p3}} e^{\hat{\xi}_{p4}\theta_{p4}} e^{\hat{\xi}_{p5}\theta_{p5}} g_{mw}(0) \quad (12)$$

where

$$\begin{aligned} \xi_{p1} &= e_5 & \xi_{p2} &= e_4 & \xi_{p3} &= e_3 \\ \xi_{p4} &= e_4 & \xi_{p5} &= e_5 \\ g_{mw}(0) &= I_{4 \times 4}. \end{aligned} \quad (13)$$

The homogeneous transform between the M and F coordinate frames (g_{mf}), W coordinates of the spherical wrists S_1 and S_2 , and M coordinates of the centers of the other two motors P_{o1} and P_{o2} are all known as they are constant.

The point at which extension of the tool arm intersects the (imaginary) plane passing through the wrists on the tool base is defined as P . Note that P has W coordinates of the form

$$p_w = [0 \quad p_{wy} \quad 0 \quad 1]^T \quad (14)$$

and (10) and (11) give

$$p_f = -(L - d)n_f + \begin{bmatrix} 0 \\ 0 \\ 0 \\ 1 \end{bmatrix} \quad (15)$$

where L is the length of the tool arm.

Lemma 2—Inverse Kinematics of the Parallel Part: The solution of the inverse kinematics of the parallel section are given by

$$p_m = g_{mf} p_f \quad (16)$$

$$\theta_{p1} = \text{atan2}(p_{mx}, p_{mz}) \quad (17)$$

$$n_m = g_{mf} n_f \quad (18)$$

$$\theta_{p2} + \theta_{p4} = \text{atan2}(-n_{my}, n_{mz} \cos(\theta_{p1}) + n_{mx} \sin(\theta_{p1})) \quad (19)$$

$$\theta_{p2} = \text{atan2} \left(p_{wy} \cos(\theta_{p2} + \theta_{p4}) - p_{my}, \frac{p_{mz}}{\cos(\theta_{p1})} - p_{wy} \sin(\theta_{p2} + \theta_{p4}) \right) \quad (20)$$

$$\theta_{p3} = \frac{\langle p_m, n_m \rangle}{-n_{my} \sin(\theta_{p2}) + n_{mx} \cos(\theta_{p2}) \sin(\theta_{p1}) + n_{mz} \cos(\theta_{p1}) \cos(\theta_{p2})} \quad (21)$$

$$l_0 = \theta_{p5}$$

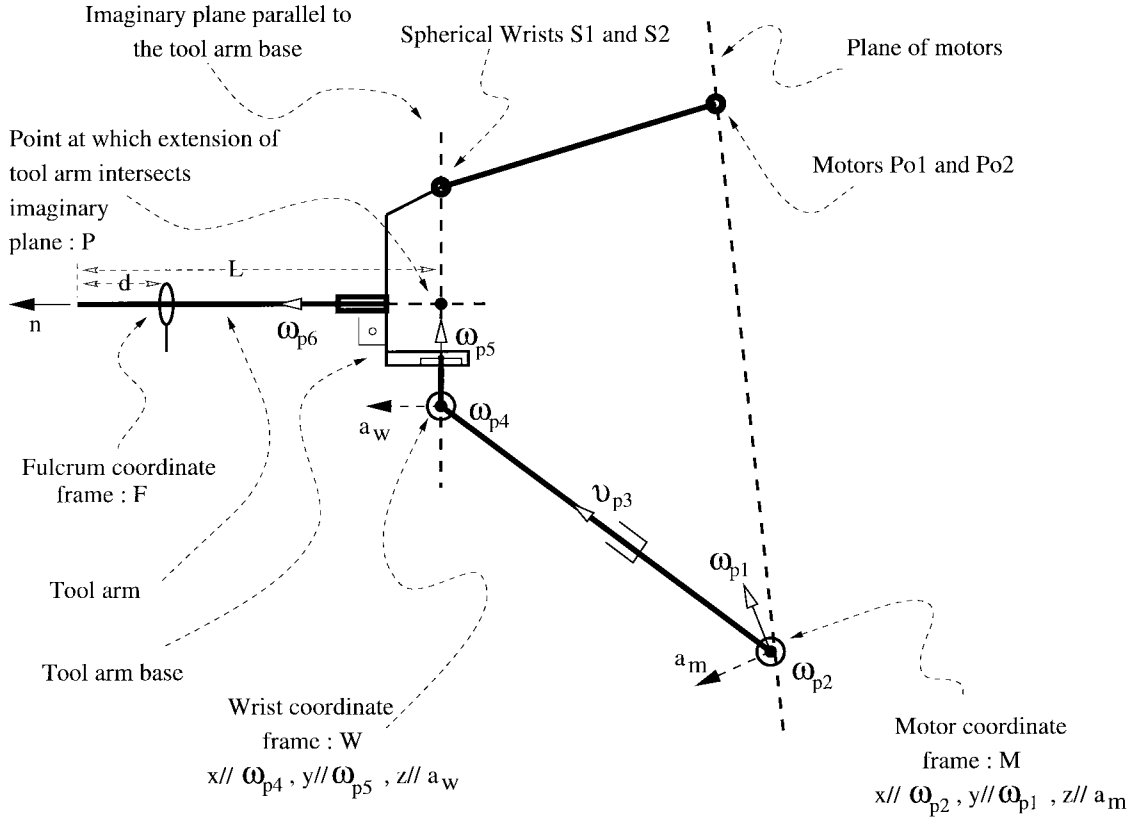


Fig. 7. Kinematic diagram of the side view of parallel section.

$$= \operatorname{atan} 2 \left(n_{mx} \cos(\theta_{p1}) - n_{mz} \sin(\theta_{p1}), \frac{-n_{my}}{\sin(\theta_{p2} + \theta_{p4})} \right) \quad (22)$$

$$l_1 = \|g_{mw} s_{1w} - p_{o1m}\| \quad (23)$$

$$l_2 = \|g_{mw} s_{2w} - p_{o2m}\| \quad (24)$$

$$\alpha = g_{mw}^{-1} e^{\hat{\xi}_{s1}\theta_{s1}} e^{\hat{\xi}_{s2}\theta_{s2}} e^{\hat{\xi}_{s3}\theta_{s3}} \begin{bmatrix} 1 \\ 0 \\ 0 \\ 0 \end{bmatrix} \quad (25)$$

$$\theta_0 = \theta_{p6} = \operatorname{atan} 2(\alpha_y, \alpha_x). \quad (26)$$

The full derivation can be found in [22]. Inverse kinematics of the parallel part have a single solution for each solution of the serial part.

B. Slave Forward Kinematics

In forward kinematics, the problem is to calculate g_{ft} , the configuration of the tool relative to the fulcrum, given θ_0 , θ_1 , θ_2 , l_0 , l_1 , and l_2 , angles of the actuated joints. Similar to the inverse kinematics calculations, the problem can be divided into two parts, first the solution for the gross stage and second the millirobot.

The gross positioning stage of the slave manipulator has a parallel structure, which complicates the solution of the forward kinematics. Usually it is not possible to find closed

form solutions for parallel manipulators.⁴ Rather, the problem is reduced to calculating the solution of a system of nonlinear algebraic equations.

In the solution of the forward kinematics of the gross positioning stage the kinematics is expressed in terms of the fulcrum coordinate frame F . The coordinate transformation between F and W is specified with the twists

$$\xi_{f1} = e_4 \quad \xi_{f2} = e_5 \quad \xi_{f3} = e_6 \quad \xi_{f4} = e_3 \quad (27)$$

and the zero configuration

$$g_{fw}(0) = \begin{bmatrix} 0 & & & \\ I_{3 \times 3} & -p_{wy} & & \\ & -L & & \\ 0 & 0 & 0 & 1 \end{bmatrix} \quad (28)$$

also shown in Fig. 8. These give the forward kinematics map

$$g_{fw}(\theta_f) = e^{\hat{\xi}_{f1}\theta_{f1}} e^{\hat{\xi}_{f2}\theta_{f2}} e^{\hat{\xi}_{f3}\theta_{f3}} e^{\hat{\xi}_{f4}\theta_{f4}} g_{fw}(0). \quad (29)$$

The linear joints give the following three constraints in the four unknowns $\theta_{f1} \cdots \theta_{f4}$

$$\left\| g_{fw}(\theta_f) \begin{bmatrix} 0 \\ 0 \\ 0 \\ 1 \end{bmatrix} - M_f \right\| = l_0 \quad (30)$$

$$\|g_{fw}(\theta_f) s_{1w} - p_{o1f}\| = l_1 \quad (31)$$

$$\|g_{fw}(\theta_f) s_{2w} - p_{o2f}\| = l_2 \quad (32)$$

⁴The most classical and well-studied example of this type of manipulators is the Stewart platform, which has no closed form solution available in literature [23].

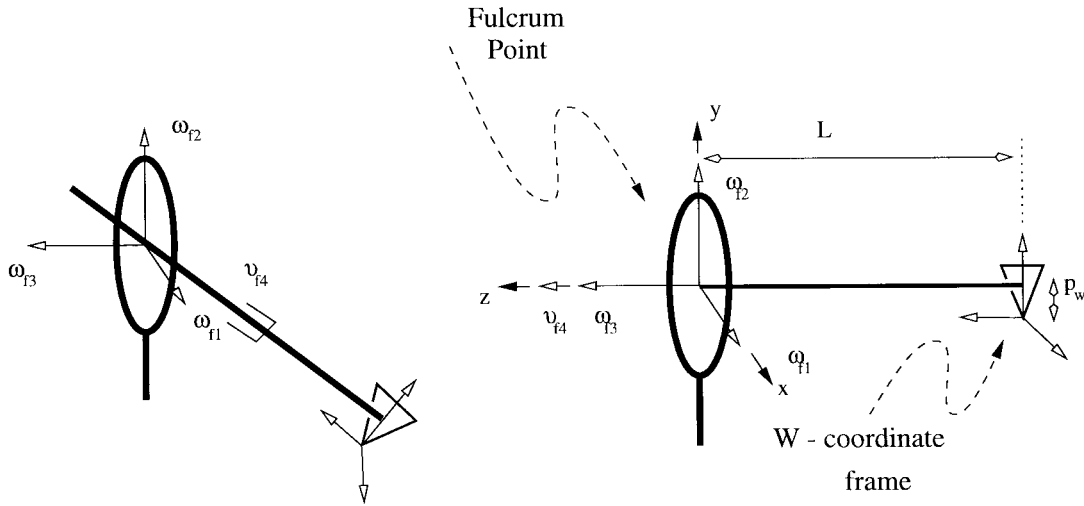


Fig. 8. Naming convention and the zero configuration for the forward kinematics of gross stage.

where point M is the center of the M coordinate frame. To solve the problem, we need to use the constraint imposed by the five DOF arm, which gives that y -axes of the W and M coordinate frames are coplanar

$$(\underline{y} \times g_{fw}\underline{y}) \parallel (\underline{y} \times (M_f - g_{fw}\underline{0})). \quad (33)$$

Equations (30)–(33) form a system of four nonlinear equations in four unknowns, which does not have a closed form solution, but can be solved numerically. For a given l_0, l_1, l_2 , there is a unique solution for $\theta_0 \dots \theta_4$.

After the gross stage forward kinematics is solved, (3) gives $g_{ft} = g_s(\theta_s)$ with

$$\theta_{s1} = \theta_{f1} \quad (34)$$

$$\theta_{s2} = \theta_{f2} \quad (35)$$

$$\theta_{s3} = \theta_{f3} + \theta_0 \quad (36)$$

$$\theta_{s4} = \theta_{f4} \quad (37)$$

$$\theta_{s5} = \theta_2 \quad (38)$$

$$\theta_{s6} = \theta_1. \quad (39)$$

1) *Workspace of the Slave Manipulator:* The workspace reachable by the gross stage of the slave manipulator is shown in Fig. 9. The boundary of the reachable workspace is determined by six surfaces corresponding to the minimum and maximum lengths of each of the three linear joints. The gross stage does not have a singularity in the workspace, but, the precision of the manipulator is reduced at the outer boundary of the workspace due to the larger moment arm.

C. Master Manipulator Forward Kinematics

The master manipulator is a simple serial structure. Using the naming convention and the zero configuration shown in Fig. 10, the kinematics of the serial part are characterized by the following twists:

$$\begin{aligned} \xi_{m0} &= -e_5 & \xi_{m1} &= e_4 & \xi_{m2} &= e_3 & \xi_{m3} &= -e_6 \\ \xi_{m4} &= [0 \quad -h \quad 0 \quad -1 \quad 0 \quad 0]^T \\ \xi_{m5} &= [h \quad 0 \quad 0 \quad 0 \quad -1 \quad 0]^T \end{aligned} \quad (40)$$

and the zero configuration

$$g_m(0) = \begin{bmatrix} I_{3 \times 3} & 0 \\ 0 & -w \\ 0 & 0 & 0 & 1 \end{bmatrix} \quad (41)$$

which gives the forward kinematics map as

$$g_m(\theta_m) = \left(\prod_{i=0}^5 e^{\xi_{mi}\theta_{mi}} \right) g_m(0). \quad (42)$$

The calculation of the body Jacobian, which is also straightforward, is not presented here due to the space limitations, but can be found in [22].

IV. CONTROL

A. Open Loop Control Issues

The main bottleneck in the dynamics of the slave manipulator is the lag in the hydraulic actuators, which is due to the transmission delay in the tubing, and the first order lag resulting from the RC effect of the tube-bladder configuration. A simple model for transmission delay in the pipes considering the compressibility of water and elasticity of tubes, but neglecting the viscous effects present, gives the propagation velocity of the pressure wave fronts as [24]

$$c = \sqrt{\frac{\frac{K}{\rho}}{1 + \frac{Kd}{Et}}} \quad (43)$$

where c is the propagation velocity, K is the bulk modulus of water, ρ is the density of water, d is the diameter of the tube, t is the thickness of the tube, and E is the linear modulus of elasticity of the tube material. The tubes connecting the manifolds to the bladders are composed of two sections. Thick section tubes have $d/t = 3.5$ and are made of Nylon 11, with $E = 0.5 \times 10^3$ psi. Thin section tubes have $d/t = 2.2$ and are made of PTFE, which has $E = 33\text{--}65 \times 10^3$ psi. Calculations

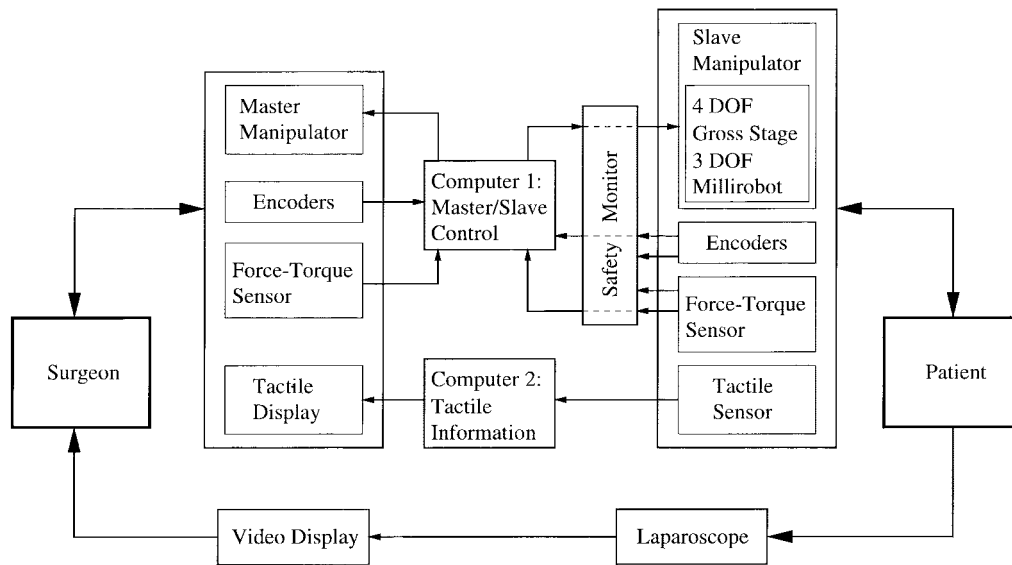


Fig. 11. Proposed control system block diagram.

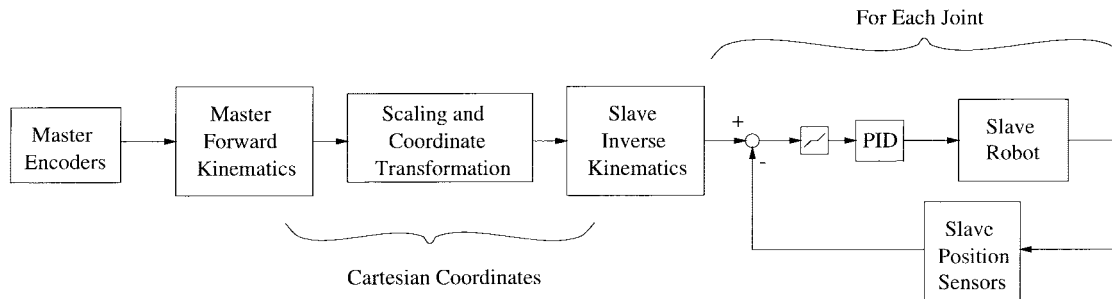


Fig. 12. Current implementation of master-slave control.

within the specifications and needs to be improved. Bandwidth and time delay for the hydraulic actuators and the noise of the analog position sensor are the limiting factors for the performance of the millirobot. Space restrictions prevented the use of a digital encoder for the roll axis, so an analog position sensor was employed instead. However, the limitations of the roll axis did not prevent the system from successfully performing the *ex vivo* suturing and knot tying tasks, as the system was being operated in master-slave mode, and the operator in the loop was easily able to compensate for the inaccuracies in the roll motion.

During the *ex vivo* experiments, suturing with a straight needle was easier compared to the curved needle due to the limited roll movement available. Although the parallel structure of the gross stage prevents the use of dynamics-based controllers, the powerful actuators used compensate for this, as can be observed from the tracking responses for the linear joints (l_0 , l_1 , and l_2).

The specifications adopted for the second version of the system are given in Table III.⁵ In addition to increasing the force and torque requirements to more easily accommodate manipulation of *in vivo* tissue, the main design changes are on the roll rotation and the wrist to gripper length. 270° of roll

rotation requirement needs to be satisfied for faster and more effective suturing. The wrist joint to gripper length is reduced to 5 cm to increase the maneuverability of the manipulator inside the abdomen.

The more comprehensive safety features not implemented in this prototype controller will be included in the later designs. The independent high level controller, which should run on a separate computer and have an independent set of sensors, is necessary for safety monitoring. The mission of this safety controller is to monitor the overall system, override commands that violate the safety constraints, and to shut down the system in case of failure. A possible low level control algorithm to avoid high interaction forces between the manipulator and the environment is discussed in Section VI-B. Increased safety must also be included in the hardware design to compensate for the potential problems in the actuator and sensor systems.

VI. CONCEPTUAL AND FUTURE ISSUES IN TELESURGERY

A. Teleoperation for Telesurgery

The main concerns for the design and control of a telesurgical system can be summarized as follows:

- 1) fidelity in force-torque feedback;
- 2) stability-fidelity trade-off;

⁵Courtesy of Endorobotics Inc.

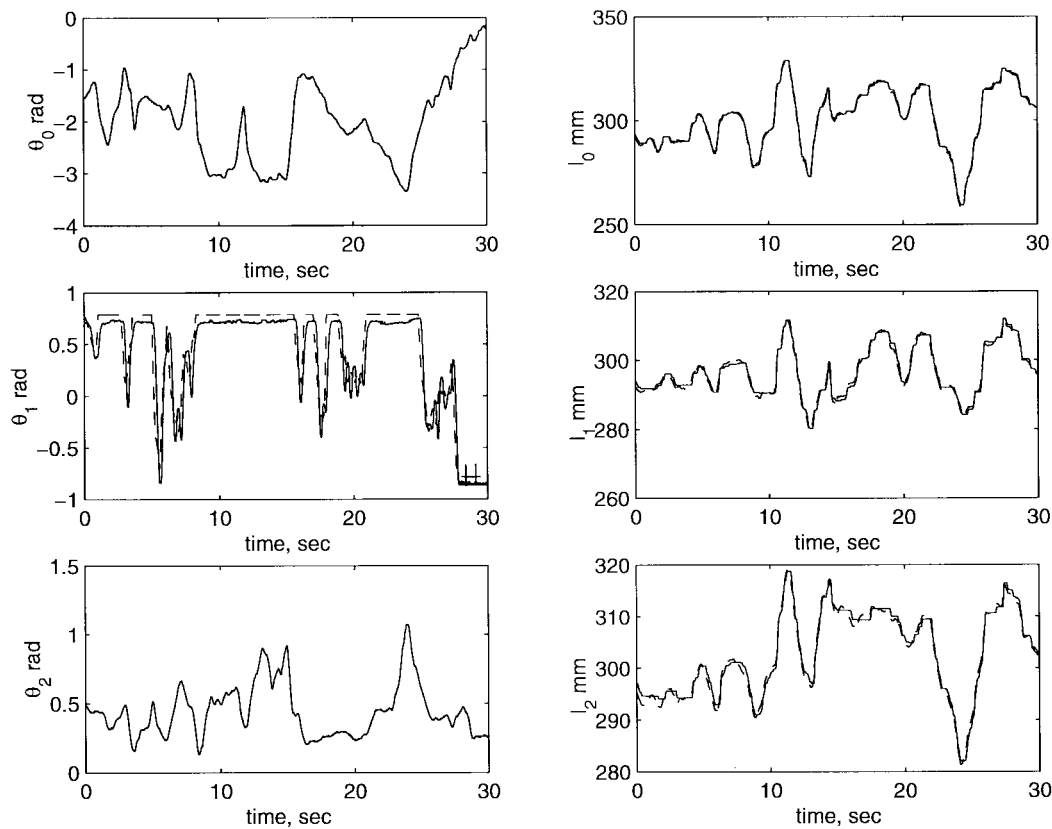


Fig. 13. Master-slave tracking response: dashed lines show the desired trajectory commanded by the master and the solid lines show the actual trajectory of the slave.

TABLE III
PERFORMANCE GOALS FOR THE SECOND VERSION OF THE MILLIROBOT

Parameter	Target Value
Wrist joint to grasper length	50 mm max
Gripping force	40 N min
Grasper opening width	8 mm min
Grasper speed: full close in	0.5 sec max
Wrist roll torque	100 N-mm min
Wrist roll range of motion	270 degrees min
Wrist roll speed	540 degrees/sec min
Wrist flexion (yaw) torque	300 N-mm min
Wrist flexion range of motion	90 degrees min
Wrist flexion speed	360 degrees/sec min
Lifetime	6 months min

3) performance under time delay

which will affect the choice of control algorithm, hardware for sensing and computation, and the limitations of the technology.

Force feedback is important for telesurgery because of the high level of interaction with the environment. Although currently there are no direct experimental results, the performance increase as a result of force feedback in conventional teleoperation tasks [25]–[27] is a clear indication, as interaction in telesurgery is more critical and delicate.

As pointed out by several authors, [28]–[31], fidelity and stability are contradicting factors in teleoperation. Control algorithms available in the literature can be classified in terms of this trade-off [31]. For example, passive communication based control algorithms of [32]–[34] are optimized for stability and

have poor fidelity [35], whereas the control algorithms of [36], [37] for ideal kinesthetic coupling are optimized for fidelity and have poor stability.

In conventional teleoperation tasks, involving manipulation of rigid objects for assembly, the interaction with the rigid environment is the main source of this stability problem. However, the challenges of telesurgery are quite different from conventional teleoperation applications. When manipulating soft tissue, stability is less of a problem while there is a significant need for fidelity during telemanipulation. It is especially important to be able to distinguish changes in environment stiffness, as with the interaction between the needle and the tissue during suturing. For example detecting when the needle enters or leaves the tissue, can only be sensed by the change in the resistance that is felt by the instrument. It is also important to be able to locate arteries and lumps hidden under tissue by feeling the changes in the stiffness of the tissue.

For increased fidelity, the performance of model based controllers will be needed, at the expense of increased computational burden. Especially, model based control (or at least gravity compensation) on the master side is critical for better fidelity and to avoid fatigue. Increased force fidelity of a force sensor on the slave, compared to position error based force feedback, might be desirable.

For operation under short time delay, the compliance of the robot and the environment would be enough for stable operation with limited kinesthetic force feedback and a safety

controller like that described in Section VI-B. The limiting factor for telesurgery under time delay will be the fidelity of teleoperation. Although the control algorithms stabilized via remote site compliance are reported to perform reasonably well for conventional teleoperation tasks, they are not satisfactory for surgery because of the lost fidelity as a result of the reduced stiffness of the manipulator. Visual aids like predictive displays will not be applicable as it is virtually impossible to fully model the environment. For larger time delays, supervisory control seems to be the only feasible solution.

It is also important to study the kinesthetic perception of the human and to optimize the teleoperation system accordingly. The coupling between the master-slave system can be chosen to minimize perceptual distortion rather than seeking an ideal response which is marginally stable and practically impossible to achieve. Also some variables of interaction can be amplified to improve sensation of manipulation for better performance. Although there are some studies in the literature on human perception in the context of teleoperation [38], there is a lot of work that should be done.

B. Hybrid Control

One way to increase safety and performance in telesurgery with time delay is to use a hierarchical controller, where the commands of the surgeon transmitted with a time delay are overlaid by a local low level controller at the remote site which guarantees safety. Hybrid control design techniques can be used to develop this low level controller to limit interaction forces under specified disturbances [39]. Such a controller can be used in a supervisory control algorithm for teleoperation under time delay to guarantee safety by eliminating excessive interaction forces.

VII. CONCLUSION

This study addressed various aspects of telesurgery. We first introduced the telesurgical workstation, a master-slave telerobotic system designed considering the special requirements of minimally invasive telesurgery, followed by its kinematic analysis, control, and experimental evaluation. Later, some conceptual and future issues in telesurgery were discussed, including discussions on teleoperation and hybrid control.

Directions for Future Work: The future work will proceed in two areas. For the Telesurgical Workstation, the proposed control algorithm will be implemented, with the force feedback and safety monitor, followed by experimental studies to further analyze the effectiveness of the robot and the control. A second robot is necessary for bimanual operation. A second version of the system is currently being developed, with modifications to improve performance based on the evaluation of the current system. This second system is being tested in animal trials at the experimental surgery laboratory at the University of California San Francisco. These results will be presented in a coming paper.

On the conceptual side, human kinesthetic perception will be experimentally studied to further identify the design goals for an effective teleoperation system design. Along this line, we are currently studying the ability of the human operator to

detect the changes in the compliance of a surface. Also, further experimental and theoretical studies are being conducted to compare alternate robot and control designs under nonideal conditions, like presence of time delay or uncertainties in the manipulator models.

REFERENCES

- [1] S. S. Sastry, M. Cohn, and F. Tendick, "Milli-robotics for remote, minimally invasive surgery," *J. Robot. Auton. Syst.*, vol. 21, no. 3, pp. 305–316, Sept. 1997.
- [2] J. Wendlandt and S. S. Sastry, "Design and control of a simplified Stewart platform for endoscopy," in *Proc. IEEE Conf. Decision Contr.*, 1994, vol. 1, pp. 357–362.
- [3] J. Wendlandt, "Milli robotics for endoscopy," Memo M94/7, Univ. California, Berkeley, Jan. 1994.
- [4] M. Cohn, L. S. Crawford, J. M. Wendlandt, and S. S. Sastry, "Surgical applications of milli-robots," *J. Robot. Syst.*, vol. 12, no. 6, pp. 401–416, June 1995.
- [5] M. B. Cohn, M. Lam, and R. S. Fearing, "Tactile feedback for teleoperation," in *Proc. SPIE*, 1993, vol. 1833, pp. 240–254.
- [6] B. L. Gray and R. S. Fearing, "A surface micromachined microtactile sensor array," in *Proc. IEEE Int. Conf. Robot. Automat.*, 1996, vol. 1, pp. 1–6.
- [7] R. S. Fearing, G. Moy, and E. Tan, "Some basic issues in teletaction," in *Proc. IEEE Int. Conf. Robot. Automat.*, 1997, vol. 4, pp. 3093–3099.
- [8] L. W. Way, S. Bhojru, and T. Mori, Eds., *Fundamentals of Laparoscopic Surgery*. London, U.K.: Churchill Livingstone, 1995.
- [9] E. Graves, *Vital and Health Statistics*, Nat. Health Survey 122, U.S. Dept. Health and Human Services, Hyattsville, MD, 1993.
- [10] F. Tendick, R. W. Jennings, G. Tharp, and L. Stark, "Sensing and manipulation problems in endoscopic surgery: Experiment, analysis and observation," *Presence*, vol. 2, no. 1, pp. 66–81, 1993.
- [11] J. W. Hill, P. S. Green, J. F. Jensen, Y. Gorf, and A. S. Shah, "Telepresence surgery demonstration system," in *Proc. IEEE Int. Conf. Robot. Automat.*, 1994, pp. 2302–2307.
- [12] R. H. Taylor, J. Funda, B. Eldridge, S. Gomory, K. Gruben, D. LaRose, M. Talamini, L. Kavoussi, and J. Anderson, "A telerobotics assistant for laparoscopic surgery," *IEEE Eng. Med. Biol. Mag.*, vol. 14, no. 3, pp. 279–288, May/June 1995.
- [13] A. Rovetta, R. Sala, X. Wen, and A. Togno, "Remote control in telerobotic surgery," *IEEE Trans. Syst., Man, Cybern. A*, vol. 26, pp. 438–443, July 1996.
- [14] F. Arai, M. Tanimoto, T. Fukuda, K. Shimojima, H. Matsuura, and M. Negoro, "Multimedia tele-surgery using high speed optical fiber network and its applications to intravascular neurosurgery—System configuration and computer networked implementation," in *Proc. IEEE Int. Conf. Robot. Automat.*, 1996, vol. 1, pp. 878–883.
- [15] R. H. Taylor, B. D. Mittelstadt, H. A. Paul, W. Hanson, P. Kazanides, et al., "An image-directed robotics system for precise orthopaedic surgery," *IEEE Trans. Robot. Automat.*, vol. 10, pp. 261–275, June 1994.
- [16] S. Lavallée, J. Troccaz, L. Gaborit, P. Cinquin, A. L. Benabid, and D. Hoffmann, "Image guided operating robot: A clinical application in stereotactic neurosurgery," in *Computer Integrated Surgery: Technology and Clinical Applications*, R. H. Taylor, S. Lavallée, G. Burdea, and R. Mösges, Eds. Cambridge, MA: MIT Press, 1995.
- [17] P. S. Schenker, H. Das, and T. R. Ohm, "A new robot for high dexterity microsurgery," in *Computer Vision, Virtual Reality and Robotics in Medicine. First International Conference, CVRMed'95 Proceedings.*, N. Ayache, Ed. Berlin, Germany: Springer-Verlag, 1995, pp. 115–122.
- [18] R. Tombropoulos, A. Schweikard, J. C. Latombe, and J. R. Adler, "Treatment planning for image-guided robotic radiosurgery," in *Computer Vision, Virtual Reality and Robotics in Medicine. First International Conference, CVRMed '95 Proceedings.*, N. Ayache, Ed. Berlin, Germany: Springer-Verlag, 1995, pp. 131–137.
- [19] P. Dario, E. Guglielmelli, B. Allotta, and M. C. Carrozza, "Robotics for medical applications," *IEEE Robot. Automat. Mag.*, vol. 3, no. 3, pp. 44–56, 1996.
- [20] R. H. Taylor, S. Lavallée, G. Burdea, and R. Mösges, Eds., *Computer-Integrated Surgery: Technology and Clinical Applications*. Cambridge, MA: MIT Press, 1996.
- [21] R. M. Murray, Z. Li, and S. S. Sastry, *A Mathematical Introduction to Robotic Manipulation*. Orlando, FL: CRC, 1994.
- [22] M. C. Çavuşoğlu, "Control of a telesurgical workstation," Tech. Rep., Memo M97/3, Electron. Res. Lab., Univ. California, Berkeley, May 1997.

- [23] K. Liu, J. M. Fitzgerald, and F. L. Lewis, "Kinematic analysis of a Stewart platform manipulator," *IEEE Trans. Ind. Electron.*, vol. 40, pp. 282–293, Apr. 1993.
- [24] D. N. Roy, *Applied Fluid Mechanics*. New York: Ellis Horwood, 1988.
- [25] H. Das, H. Zak, W. S. Kim, A. K. Bejczy, and P. S. Schenker, "Operator performance with alternative manual control modes in teleoperation," *Presence*, vol. 1, no. 2, pp. 201–218, Spring 1992.
- [26] W. S. Kim, B. Hannaford, and A. K. Bejczy, "Force-reflection and shared compliant control in operating telemanipulators with time delay," *IEEE Trans. Robot. Automat.*, vol. 8, pp. 176–185, Apr. 1992.
- [27] B. Hannaford, L. Wood, D. A. McAfee, and H. Zak, "Performance evaluation of a six-axis generalized force-reflecting teleoperator," *IEEE Trans. Syst., Man, Cybern.*, vol. 21, pp. 620–633, May/June 1991.
- [28] B. Hannaford, "A design framework for teleoperators with kinesthetic feedback," *IEEE Trans. Robot. Automat.*, vol. 5, pp. 426–434, Aug. 1989.
- [29] ———, "Stability and performance tradeoffs in bi-lateral telemanipulation," in *Proc. IEEE Int. Conf. Robot. Automat.*, 1989, pp. 1764–1767.
- [30] G. J. Raju, G. C. Verghese, and T. B. Sheridan, "Design issues in 2-port network models of bilateral remote manipulation," in *Proc. IEEE Int. Conf. Robot. Automat.*, 1989, pp. 1316–1321.
- [31] D. A. Lawrence, "Stability and transparency in bilateral teleoperation," *IEEE Trans. Robot. Automat.*, vol. 9, pp. 624–637, Oct. 1993.
- [32] G. Niemeyer and J. J. E. Slotine, "Stable adaptive teleoperation," *IEEE J. Oceanic Eng.*, vol. 16, pp. 152–162, Jan. 1991.
- [33] R. J. Anderson and M. W. Spong, "Bilateral control of teleoperators with time delay," *IEEE Trans. Automat. Contr.*, vol. 34, pp. 494–501, May 1989.
- [34] ———, "Asymptotic stability for force reflecting teleoperators with time delay," *Int. J. Robot. Res.*, vol. 11, pp. 135–148, Apr. 1992.
- [35] C. A. Lawn and B. Hannaford, "Performance testing of passive communication and control in teleoperation with time delay," in *Proc. IEEE Int. Conf. Robot. Automat.*, 1993, pp. 776–783.
- [36] Y. Yokokohji and T. Yoshikawa, "Bilateral control of master-slave manipulators for ideal kinesthetic coupling—Formulation and experiment," in *Proc. IEEE Int. Conf. Robot. Automat.*, 1992, pp. 849–858.
- [37] ———, "Bilateral control of master-slave manipulators for ideal kinesthetic coupling—Formulation and experiment," *IEEE Trans. Robot. Automat.*, vol. 10, pp. 605–620, Oct. 1994.
- [38] L. A. Jones and I. W. Hunter, "Analysis of the human operator controlling a teleoperated microsurgical robot," in *Proc. 6th IFAC/IFIP/IFORS/IEA Symp. Anal., Design Evaluation Man-Machine Syst.*, 1995, pp. 593–597.
- [39] M. C. Çavuşoğlu, J. Yan, and S. S. Sastry, "A hybrid system approach to contact stability and force control in robotic manipulators," in *Proc. 12th IEEE Int. Symp. Intell. Contr. (ISIC'97)*, July 1997, pp. 143–148.



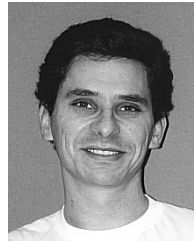
Murat Cenk Çavuşoğlu received the B.S. degree from Middle East Technical University, Ankara, Turkey, in 1995, the M.S. degree from the University of California, Berkeley, in 1997, and is currently pursuing the Ph.D. degree at the Electrical Engineering and Computer Sciences Department, University of California, Berkeley.

His research interests are medical robotics, virtual environments for training, and control systems.



Frank Tendick received the B.S. degree in aeronautics and astronautics from the Massachusetts Institute of Technology, Cambridge, the M.S. degree in mechanical engineering from the University of California, Berkeley, and the Ph.D. in bioengineering from the joint program at the University of California, San Francisco, and Berkeley campuses.

He is now an Assistant Professor in the Department of Surgery, University of California, San Francisco, and the Department of Bioengineering, University of California, Berkeley. His interests are in human-machine interfaces, teleoperation, and virtual environments, especially as applied to surgery.



Michael Cohn received the Ph.D. degree from the Department of Electrical Engineering and Computer Sciences, University of California, Berkeley.

He is currently with Endorobotics, Inc., Berkeley, CA, and also working as a Post-Doctoral Researcher at the Berkeley Sensor and Actuator Center, University of California, Berkeley.



S. Shankar Sastry received the Ph.D. degree from the University of California, Berkeley, in 1981.

He was on the faculty of the Massachusetts Institute of Technology (MIT), Cambridge, from 1980 to 1982 and Harvard University, Cambridge, MA, as a Gordon McKay Professor in 1994. He is currently a Professor of Electrical Engineering and Computer Sciences and Director of the Electronics Research Laboratory, University of California, Berkeley. He has held visiting appointments at the Australian National University, Canberra, the University of Rome, Scuola Normale, and University of Pisa, the CNRS Laboratory LAAS in Toulouse, and as a Vinton Hayes Visiting Fellow at the Center for Intelligent Control Systems at MIT. His areas of research are nonlinear and adaptive control, robotic telesurgery, control of hybrid systems, and biological motor control. He is a coauthor of *Adaptive Control: Stability, Convergence and Robustness* (Englewood Cliffs, NJ: Prentice-Hall, 1989), *A Mathematical Introduction to Robotic Manipulation* (Orlando, FL: CRC, 1994), and the author of *Nonlinear Control: Analysis, Stability* (New York: Springer-Verlag, 1999). He coedited *Hybrid Control II* and *Hybrid Control IV*, and *Hybrid Systems: Computation and Control* Springer Lecture Notes in Computer Science, 1995, 1997, and 1998.

Dr. Sastry received the President of India Gold Medal in 1977, the IBM Faculty Development award for 1983–1985, the NSF Presidential Young Investigator Award in 1985, and the Eckman Award of the American Automatic Control Council in 1990. He was an Associate Editor of the *IEEE TRANSACTIONS ON AUTOMATIC CONTROL*, *IEEE Control Magazine*, *IEEE TRANSACTIONS ON CIRCUITS AND SYSTEMS*, and the *Journal of Mathematical Systems, Estimation and Control* and is an Associate Editor of the *IMA Journal of Control and Information*, the *International Journal of Adaptive Control and Signal Processing* and the *Journal of Biomimetic Systems and Materials*.